

Automated classification of cellular images obtained on the ImageStream imaging flow cytometer.



George TC, Venkatachalam V, Hall BE, Henery SM, Friend SL, Zimmerman C, Basiji DA, Ortyrn WE, Morrissey PJ. Amnis Corp., 2505 3rd Ave, Suite 210, Seattle, WA 98121. www.amnis.com

Abstract

The human brain can rapidly differentiate cells with very subtle differences in their imagery. However, manual classification suffers from a lack of objectivity, repeatability, and reportability, and such per-cell subjectivity makes it difficult to identify subtle changes in large populations of cells. Automated classification specifically addresses these limitations. By identifying and combining 1000s of specific discriminatory characteristics of large numbers of cell images per sample, we can obtain results that are highly objective, repeatable, statistically significant and scalable with data size. Here we describe and apply a novel automated classification technique to several biological applications, including the classification of whole blood cells and to the discrimination of mitotic, apoptotic and live cells. Large event image files are collected on the ImageStream, a high speed imaging flow cytometer (Amnis Corporation) which automatically collects large numbers of images per data set and provides quantitative image analysis tools. These tools include custom masks (identifying specific parts of images) and features based on image characteristics such as shape, size, signal strength and texture. Our automated classification paradigm utilizes a modification of Fisher's Linear Discriminant criterion to measure the ability of our custom masks and features to discriminate the cells of interest. A single classifier output feature is then created that is the specific linear combination of features and masks that provide maximum discrimination. Thus, our method collapses a multi-parameter classification onto a simple histogram, which can be readily conceptualized and reported. The classification scheme can be adapted to use only specific categories of features/masks and specific images (fluorescent, darkfield or brightfield). It can also be applied to multiple classes of cells. The data presented demonstrate the application of a novel automated cell classification method to the discrimination of cells within large cellular image data sets collected on the ImageStream.

Introduction

Image-based classification enables grouping of cells with similar morphologic characteristics that exist within heterogeneous samples. This allows for identification of cells from different lineages, cells that have responded to treatment, and/or cells that are in a particular stage of development or cycle. The ImageStream high speed quantitative image cytometer routinely collects large event image files and quantifies 1000s of image-based characteristics of each cell, enabling objective and statistically robust cell classification. Statistical computational methods can be applied that convert multi-dimensional biological input data into classification outputs. Here we apply a modification of the Fisher's Linear Discriminant method to create single output features that differentiates specific cell populations within heterogeneous samples. Here we create and utilize classifiers that a) identify the different phases of mitosis, b) sub-classify neutrophils on the basis of lobe structure, c) discriminate cell conjugates from fusions, and d) track morphologic changes associated with pseudopod formation.

Materials and Methods

Nuclear staining for mitotic cell classification:

THP-1 human monocytic cells were cultured in 5% FBS-supplemented RPMI at 37 C, 5% CO2 and harvested at mid-exponential growth, washed, fixed in 1% formaldehyde/PBS for 10 minutes at room temperature. The cells were then washed and resuspended in 0.1% TritonX100/PBS containing 20 μM DRAQ5 (Biosstatus) and run on the ImageStream.

Pseudopod formation and PODO staining:

FDCP-1 myeloid progenitor cells were incubated with the chemoattractant IL-3 to induce pseudopod formation for the indicated times at 37 C. The cells were washed, stained on ice with PE conjugated anti-PODO, then washed, resuspended in 1% formaldehyde/PBS and run on the ImageStream.

Conjugate / Fusion formation

Human PBMC were incubated with ptk26-labeled tumor cells for the indicated times at 37 C. The cells were washed in wash buffer (2%FCS/PBS) and stained in wash buffer with surface markers to pDC (FITC anti-BDCA-2 and BDCA-4, and PE-Cy5 anti-CD123) for 20' at 4C. After washing, the cells were fixed in 1% Formaldehyde/PBS containing 7-AAD (40 μM) and run on the ImageStream.

Nuclear staining for human neutrophil sub-classification:

Human blood was collected in K3 EDTA lavender top vacutainer tubes and incubated in 10X volume of FACS-lyse (BD) for 10 minutes at room temperature to lyse RBCs and fix the WBC. The cells were washed twice, resuspended in PBS containing DRAQ5 (20 μM) and run on the ImageStream.

Image acquisition and analysis:

Image files were automatically acquired in flow using the ImageStream imaging flow cytometer. Single color controls were used to calculate a spatial cross-talk matrix that was applied to the image files in order to isolate probed images to single imaging channels. The resulting compensated image files were analyzed using image-based algorithms available in the IDEAS statistical analysis software package.

Cell Classification from multi-dimensional data:

Our classification routine processes thousands of input parameters to create a single output feature (a "classifier") that identifies a particular cell type the user has chosen. This classifier can be used to find cells of similar characteristics both within a file as well as in all files in an experiment. The effectiveness of the classifier depends on: a) the quality of the example cells ("truth") selected to train the classifier; b) the specific inclusion of discriminatory parameters; and c) the method of combining the chosen parameters into a single output. Our classification method can be broken into three steps: 1) Selection of "truth": The user supplies a hand-selected set of example cells of interest ("truth" population). These cells should span the range of acceptable examples. Multiple truth populations can be selected for each file. 2) Characteristic evaluation process (automated): All features are normalized to the same scale ($\mu = 0 \pm 1$). The classification routine sorts through the measured characteristics to select those which best separate the truth population from the rest of the cells in the file. The discriminating power of a feature is high when inter-class variance is maximized and intra-class variance is minimized. We use the Fisher's Discriminant Ratio (Rd), which is the difference in feature mean values between truth and non-truth (inter-class variance) divided by the sum of the feature standard deviations of truth and non-truth (intra-class variance), to quantify the separating power of each feature. Features that improve separation are chosen for the next step. 3) - Combination of the chosen features (automated) - we Linear Discriminant Analysis to combine all the chosen features with appropriate weighting into a single classifier.

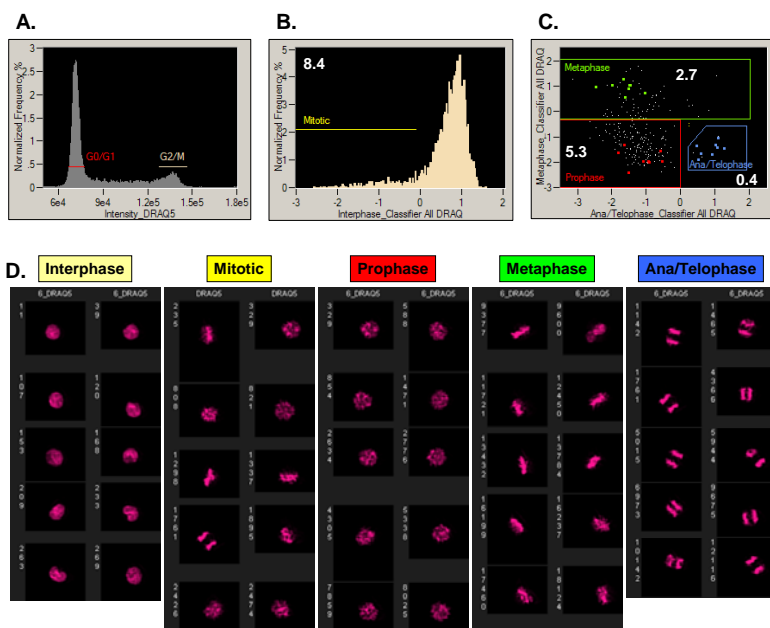


Figure 1: Classification of Mitotic events using nuclear imagery

The phases of mitosis can be distinguished from one another on the basis of nuclear morphology. Here we applied the classifier to identify prophase, metaphase, and anaphase/telophase THP-1 cells. Single cells were identified by gating on events with intermediate brightness and high aspect ratio (data not shown). Single cells with 4N DNA content are gated (G2/M) on the DRAQ5 intensity histogram (A). Based on visual inspection of the DRAQ5 nuclear imagery, five example cells of each discernable population (interphase, prophase, metaphase, and anaphase/telophase) within the G2/M gate were chosen as truth populations. These truth populations were used to create respective classifiers that were subsequently used to identify each group. Note that in this experiment, the classifier was limited to include only features calculated from the DRAQ5 image. Mitotic events have low Interphase Classifier values and are gated in (B). The percentage of G2/M cells that are mitotic is indicated on the plot. The three remaining populations can be identified by plotting the Anaphase/Telophase Classifier vs. the Metaphase Classifier for Mitotic events (C). Prophase cells score low for both features, metaphase cells score high for the Metaphase classifier, and anaphase/telophase score high for the Anaphase/Telophase Classifier and low for the Metaphase Classifier. The percentage of G2/M cells that each population represents is indicated on the plot. Representative DRAQ5 images from each of the gated populations are shown in (D).

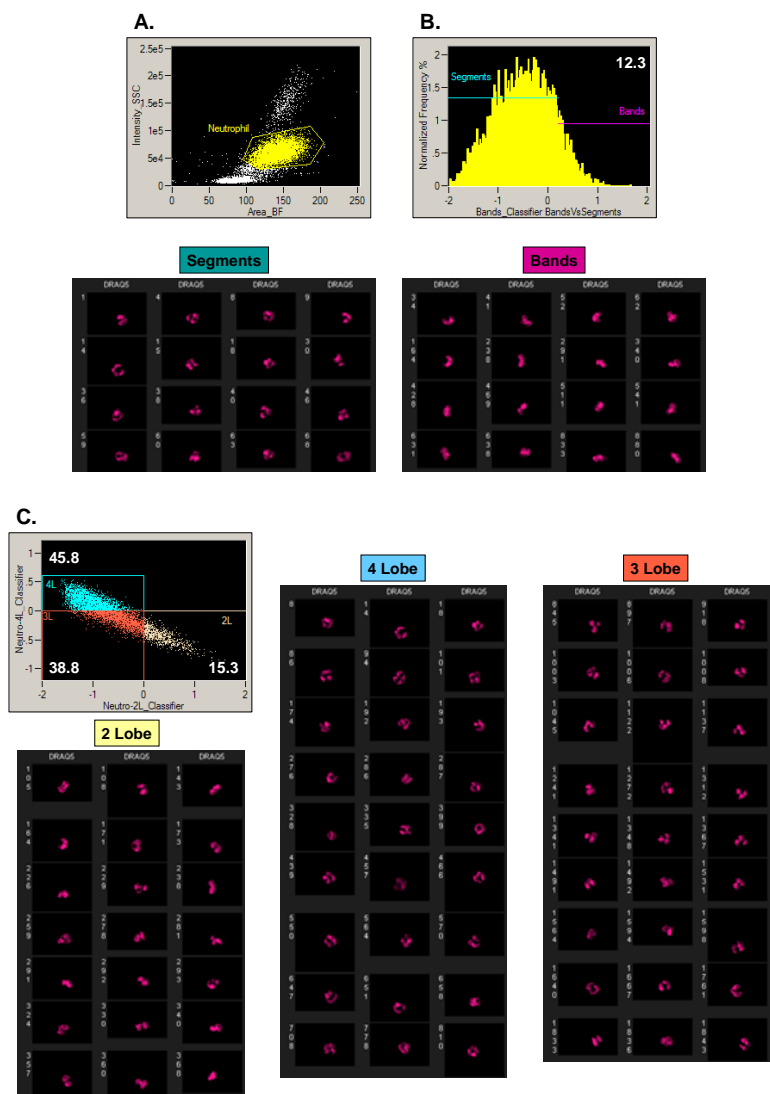


Figure 2: Sub-classification of human peripheral blood neutrophils using nuclear imagery

Here we applied the classifier to identify peripheral blood neutrophil sub-populations on the basis of nuclear morphology. Single leukocytes were identified by gating on events with normal DNA content to eliminate anucleated debris and doublets (data not shown). Neutrophils were identified as high SSC large area cells (note that the very high SSC cells are eosinophils) in (A). Ten example segmented neutrophils and eleven example banded neutrophils were chosen as truth populations to create respective classifiers that were subsequently used to identify each group. Note that in this experiment, the classifier was limited to include only features calculated from the DRAQ5 image. Banded neutrophils have high Band Classifier values (and conversely, segmented neutrophils have low Band Classifier values) and are gated in (B). The percentage of neutrophils that are banded is indicated on the plot. Representative banded and segmented neutrophil DRAQ5 images are shown below the plot. To classify neutrophils based on nuclear lobicity, we selected five examples each of neutrophils that appeared to have two, three, or four nuclear lobes. Plotting the resultant 2 Lobe Classifier vs. 4 Lobe Classifier revealed a continuum that was gated into three populations (C). Bilobed neutrophils had high 2 Lobe and low 4 Lobe scores, four-lobed neutrophils had the opposite phenotype, while three-lobed neutrophils had low values for both classifiers. The relative percentage of each lobe population is indicated on the plot, and representative DRAQ5 images from each population are shown.

Conclusion

Here we describe and demonstrate the application of an automated classification method to discriminate cells based on their appearance using parameter-rich image data collected using ImageStream high speed image cytometry. This approach is ideally suited to classification problems that do not lend themselves to single parameter discrimination. The method combines multiple relevant discriminatory features, appropriately weighted, into a single linear classifier that can be used to identify cells that look like the corresponding hand-selected truth population. Once created, these classifiers are invariant parameters and can be applied to all samples within an experiment. We used the classifier to a) enumerate prophase, metaphase, and anaphase/telophase events, b) sub-classify neutrophils into bands, segments, and different lobe counts, c) distinguish between cell fusions and cell-cell conjugates and measure the time-dependent increase in fusion formation, and d) track the kinetics of IL-3 induced PODO capping and pseudopod formation in myeloid progenitor cells. To highlight one example from this study, no single parameter adequately distinguishes banded and segmented neutrophils. Of interest would be to use the classifiers described here to measure the shift in neutrophil phenotype that occurs during bacterial infections or leukemic conditions. This method also holds promise in the morphologic classification of blood and bone marrow samples, and in combination with surface immunophenotyping, should enable more accurate and detailed classification schemes.

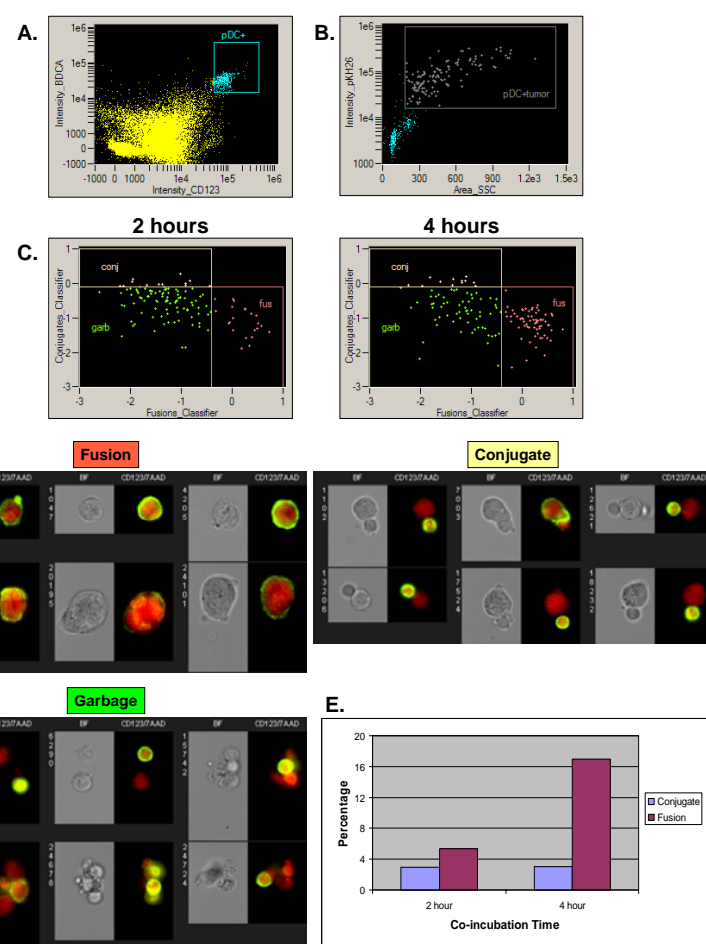


Figure 3: Classification of conjugate and fusion events

Cell-cell interaction can result in conjugate formation or cellular fusion. Here we applied the classifier to distinguish plasmacytoid dendritic cell (pDC)-tumor cell conjugates from pDC-tumor fusions. pDC were incubated with ptk26-labeled tumor cells for 2 or 4 hours, then stained with surface pDC markers (BDCA and CD123) and 7-AAD and run on the ImageStream. Events stained with both pDC marker are gated in (A), and those with large area and ptk26+ staining are further gated in (B). The events in this gate included pDC-tumor conjugates, pDC-tumor fusions, and nonspecific cell clumps ("garbage"). Six example images of each population were chosen as truth populations to create respective classifiers that were subsequently used to identify each group. Fusions have high Fusion Classifier scores and low Conjugate Classifier values, conjugates have the opposite phenotype, and cell clumps (garbage) score low with both classifiers (C, representative images shown in D). The percentages of cells in the pDC gate that are fusions or conjugates are plotted in the bar graph (E).

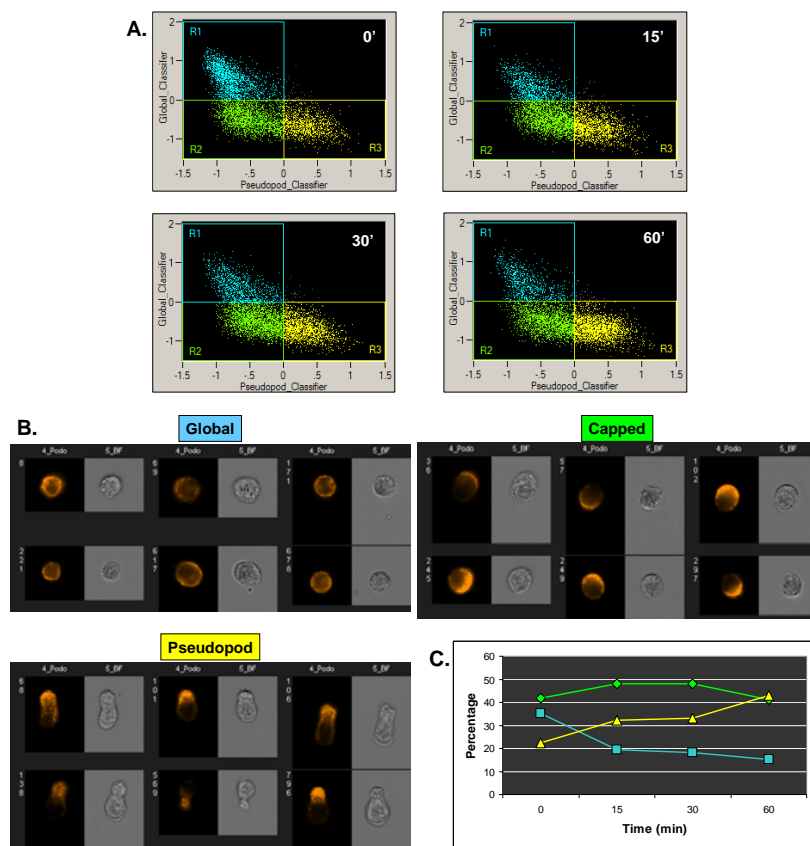


Figure 4: Kinetics of chemoattractant-induced capping and pseudopod formation

FDCP-1 myeloid progenitor cells form prominent pseudopods when exposed to the chemoattractant IL-3. During this process, surface PODO caps to one side of the cell before co-distributing with the emerging pseudopod. In this experiment, we sought to measure the kinetics of IL-3-induced PODO capping and pseudopod formation in these cells. To do this, we classified the FDCP-1 cells into three groups: 1) round cells with PODO globally distributed around the cell ("Global"); 2) round cells with capped PODO ("Capped"); and 3) elongated cells ("Pseudopods"). Six example images of each population were chosen as truth populations to create respective classifiers that were subsequently used to identify each group. Global cells have high Global Classifier scores and low Pseudopod Classifier values, pseudopod-containing cells have the opposite phenotype, and cells with capped PODO score low with both classifiers (A, representative images shown in B). The percentages of cells of each class (global in blue, capped in green, pseudopod in yellow) at the indicated IL-3 incubation time points are plotted in the line graph (C). We observed a rapid increase in capped and pseudopod cells after 15 minutes of IL-3 incubation that continued over the course of one hour.